Springer

Journal of
Mechanical
Science and
Technology

Journal of Mechanical Science and Technology 22 (2008) 1305~1312

www.springerlink.com/content/1738-494x

Suggestion of MSTV (Modified-Stick-Transition-Velocity) model for hysteretic damping mechanism

Jae-Cheol Lyu[1], Gyung-Hun Nho[1], Bo-Sun Chung[1], Jeong-Han Lee[2], Sung-Woon Jung[2] and Wan-Suk Yoo[2,*]

[1]*Washing Machine Division, Digital Appliance Company, LG Electronics, Changwon city, Gyeongnam, 641-713, Korea*

[2]*Graduate student, School of Mechanical Engineering, Pusan National University, Busan, 609-735, Korea*

(Manuscript Received August 6, 2007; Revised October 9, 2007; Accepted April 4, 2008)

Abstract

To decrease vibration and noise in washing machines, lubricated friction dampers were installed. Although the structure of the friction damper is simple, it was not easy to develop a mathematical model for the dynamic behavior of the lubrication damper. To see the dynamic behavior of a friction damper, physical tests were carried out via a material testing machine by changing exciting amplitudes and frequencies. Complicated curves of spring characteristics and damping showed a hysteretic behavior. In this paper, a reasonable model for a friction damper is suggested. To model the hysteretic behavior of a friction damper, a Coulomb friction model was first applied. To get a refined model for stick and transition, an STV (stick transition velocity) model was analyzed. To develop a more accurate mathematical model, an MSTV (modified stick transition velocity) model was proposed. In the MSTV model, the friction force could be changed due to the velocity of the damper, and the damping force was calculated according to the relative velocity between the external displacement and the deformation of the sponge in the friction damper. The MSTV model was in a good agreement with the experimental results.

Keywords: Friction damper; Physical experiments; STV (Stick Transition Velocity); MSTV (Modified Stick Transition Velocity)

1. Introduction

Washing machine development to automatic washing machines occurred with several milestones. The introduction of electric motors, synthetic detergents, spin and dry features, steel drums and plastic drums, and application of microprocessors are turning points in developing washing machines [1]. Automatic washing machines are divided into two types according to loading types, i.e., top loading model with vertical axis and front loading type with horizontal axis [2]. Front loading type became standard in Europe, and top loading models were popular in America and Asia. In the top loading model, agitator type has been popular in the United States, and pulsator type has been used in Asia. Recently, front loading has been increasing in the United States and Asia.

To reduce vibration and oscillatory walk, two types of dynamic balancer have been widely used. A hydraulic balancer composed of fresh water, salt water, oil, or liquid mercury, was more effective than a solid balancer [3]. The effect of lengths of suspending rods, attaching angles, vertical and horizontal position, stiffness of spring on the change of vibration were also studied [4]. Another mathematical model was developed for the dynamic analysis of the vertical axis automatic washing machines of pulsator type [5]. Ball type solid balancer was also used to reduce the vibration caused by unbalance of rotor [6]. They found that the friction between balls and race and the deviation between geometric center and rotation cen-

*Corresponding author. Tel.: +82 51 510 1457, Fax.: +82 51 581 8514
E-mail address: wsyoo@pusan.ac.kr
DOI 10.1007/s12206-008-0406-9

ter of drum need to be minimized to maximize the effect of a balancer. The advantage of an air damper in automatic washing machine was studied by [7], who presented an analytical approach and an application for designing non-viscous air damper with a piston and a cylinder.

Since the amount of unbalanced mass depends on both the mass of laundry and the washing mode, it is almost impossible to formulate mathematically. Thus, most of the vibration reduction techniques for washing machines depend on physical experiments. To reduce the number of experiments, an optimal design method using a response surface method for dynamic characteristics of a washer was presented [8]. In their proposed method, an orthogonal array was used to obtain best cases for minimum number of experimentation. Using these experimental values, optimal design was performed by using a response surface method.

To reduce vibrations in a washing machine, several types of dampers have been used. If the cost is not critical, an expensive and complicate damper could be designed by using a well-developed technology in the automobile industry. The bushing element used in a vehicle suspension could be adopted in a washing machine, which shows nonlinear characteristics for both displacements and frequencies and hysteretic responses for the repeated vibration excitations. Since the characteristics of the rubber bushing affects significantly the accuracy of the dynamic simulation results, it should be taken account in the washing machine model. Thus, the type of the hysteretic restoring force cannot be expressed by an algebraic function of the instantaneous displacement and velocity. This history-dependent characteristic of a bushing renders the hysteretic systems more difficult to model and analyze than other non-linear systems [9, 10].

An inexpensive damper model in a washing machine usually adopts a friction damper lubricated with a sponge. This friction damper exerts different friction forces depending on stick behavior in the contacting surface. Several models for the friction damper have been proposed [11] and [12]. Liang [11] simply adopted a Coulomb friction model, and Wee [12] analyzed a two-dimensional stick-slip model for the shear force occurring in the rubber. Ok [13] analyzed frequency and amplitude characteristics of the rubber bushing with a Bouc-Wen model. Yoo [14] compared a computer simulation and physical experiment of a drum-type washing machine with a friction damper. To match the simulation results to measured data, a damping characteristic depending on amplitudes and frequencies were measured and applied. But, any simple mathematical models could not be applied for the friction damper used in a washing machine.

2. Real tests of friction damper

2.1 Structure of friction damper

In Fig. 1, a drum type washing machine used in this research is shown [14]. The tub is connected to a cabinet with two springs and three dampers. Two springs are installed in the upper part of the tub, and two dampers are installed in the bottom side and another damper is on rear side.

In Fig. 2, a detailed schematic of the friction damper used in the washing machine is shown. Body 1, 2, 3, 4, and 5 in Fig. 2 represents outer tube, inner tube, sponge, rubber bushing, and orifice, respectively. Sponge is lubricated with grease and exerts a frictional damping force between the inner tube and outer tube. During the motion of the damper, air flow in the orifice also exerts an air resistance. The rubber mount helps to connect the damper to the drum and to reduce the vibration.

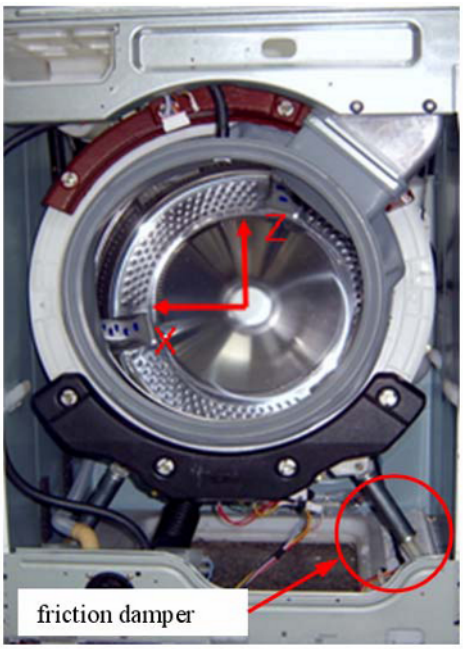

Fig. 1. Drum-type washer and its friction damper.

Table 1. Frequency and displacement in harmonic test.

Frequency f [Hz]	Displacement δ_i [mm]
1.0	0.3, 0.5, 1.0, 5.0, 10.0
3.0	0.3, 0.5, 1.0, 3.0, 5.0
6.67	0.3, 0.5, 1.0, 1.5
10.0	0.3, 0.5, 1.0, 1.5

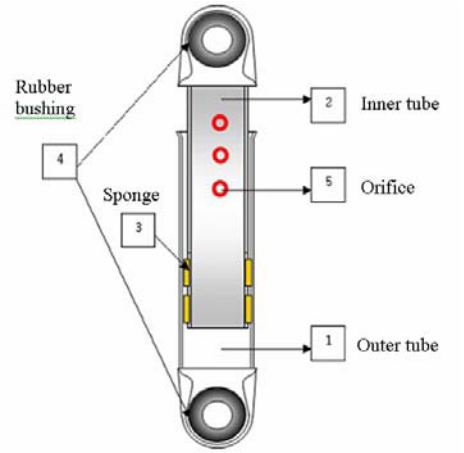

Fig. 2. Components in a friction damper.

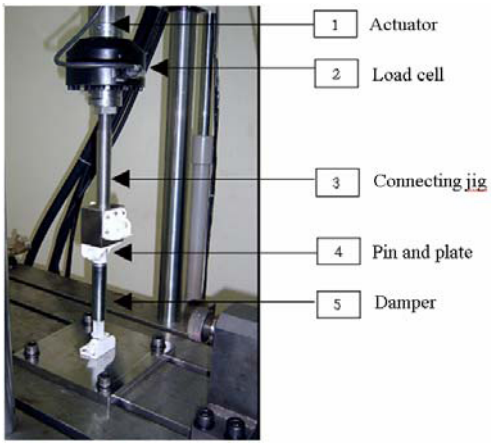

Fig. 3. Damper with a jig in testing machine.

2.2 Testing procedure

A uni-axial testing system made from MTS (2005) was used to test the friction damper, as shown in Fig. 3. The system generates the maximum force of 100kN, and the maximum stroke of 84 mm. Harmonic input tests were carried out to determine stiffness and damping characteristics of the friction damper as a function of displacement and frequency. The harmonic input was applied for several different

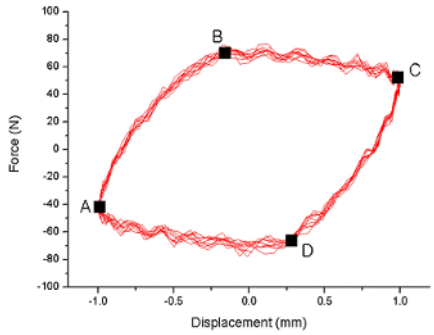

Fig. 4. Force versus displacement (10Hz, 1mm).

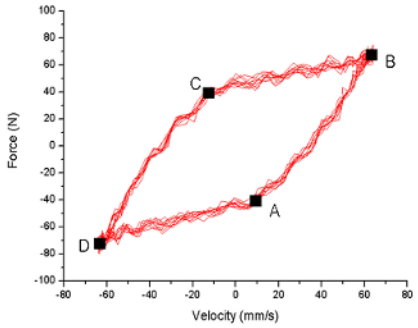

Fig. 5. Force versus velocity (10Hz, 1mm).

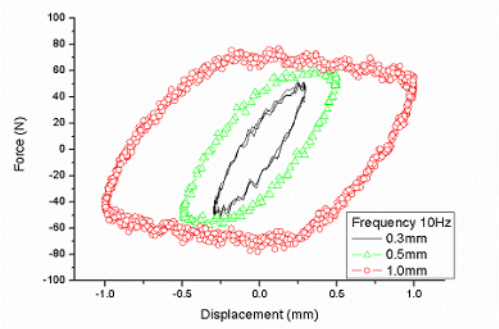

Fig. 6. Forces versus amplitudes (frequency of 10Hz).

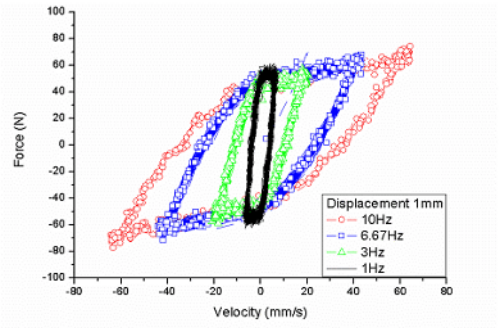

Fig. 7. Forces versus frequencies (amplitude of 1mm).

frequencies and displacements, shown in Table 1, which can be represented as:

$$\delta(t) = \delta_i \sin 2\pi ft \tag{1}$$

2.3 Experimental results

Fig. 4 and Fig. 5 show the force change due to velocity and displacement with a displacement of 1mm and frequency of 10Hz, respectively. The loading sequence starts from A and makes a loop to B-C-D. As shown in Fig. 4 and Fig. 5, the characteristic of friction force clearly shows a hysteretic behavior. In the AB region, the exciting velocity of the damper is increasing and the damping force is also increasing, where the velocity reaches at a maximum at point B. In the BC region, the velocity is decreasing, and the velocity of the sponge becomes zero at point C. The CD region and the DA region are reverse states of the AB and BC, respectively.

Fig. 6 shows the forces due to amplitude change with a frequency of 10Hz, and Fig. 7 shows the forces due to frequency change with frequency of 10Hz. As shown in Fig. 6 and Fig. 7, the characteristic of friction force shows quite different hysteretic behavior depending on frequency and amplitude. A smaller amplitude makes the smaller hysteretic loop, and A higher frequency also makes a stiffer loop.

3. Conventional modeling of friction damper

3.1 A mathematical model of a friction damper

To develop a mathematical model for the frictional damper, the damper system in Fig. 2 is modelled as a combination of spring and damper as shown in Fig. 8. In Fig. 8, Y(t) and X(t) are displacements of external displacement and displacement of the sponge, respectively. Two masses M and m, represent the mass of the jig and the mass of the moving part in the damper, respectively. The force due to deformation of the sponge is assumed a linear spring and damper, which has a stiffness of k_1 and a damping coefficient of c_1. Air resistance invoked from the airflow through the hole is modelled as a damper with damping coefficient of c_2. The force f_{fric} represents the friction force occurring on the sponge and the outer tube.

The equations of motion for the system shown in Fig. 8 can be derived as shown in Eq. (2) and Eq. (3), where F(t) is the force applied on the jig to activate the vibration. To model the frictional damping force f_{fric}, the following three different models are compared: Coulomb friction model in section 3.2, STV (stick transition velocity) model in section 3.4, and MSTV (modified stick transition velocity) model in chapter 4.

$$M\ddot{Y}(t) + c_1\dot{Y}(t) + k_1Y(t) = F(t) + c_1\dot{X}(t) + k_1X(t) \tag{2}$$

$$m\ddot{X}(t) + (c_1 + c_2)\dot{X}(t) + k_1X(t) = c_1\dot{Y}(t) + k_1Y(t) + f_{fric} \tag{3}$$

3.2 Coulomb friction model

A Coulomb friction model shown in Fig. 9 was applied for the friction force of the sponge. The mathematical model was written as shown in Eq. (4). The $f_{\max}$ value in Eq. (4) was determined from experimental results.

$$f_{fric} = \begin{bmatrix} -sign\left|\dot{X}(t)\right| f_{\max} & when \quad \dot{X}(t) \neq 0 \\ 0 & when \quad \dot{X}(t) = 0 \end{bmatrix} \tag{4}$$

3.3 Parameter identification for coulomb model

With the Coulomb friction model shown in Fig. 9, the stiffness and damping coefficient are chosen by an

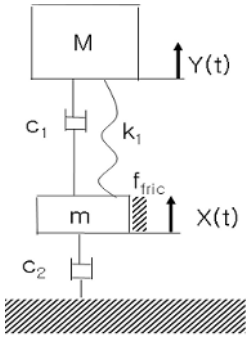

Fig. 8. Mathematical model of a friction damper.

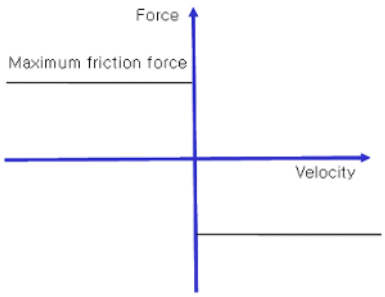

Fig. 9. Coulomb friction model.

optimization technique to minimize the difference between the measured data and analytical data. For the optimization, the objective function was selected as:

Minimize error

$$E = \sqrt{\frac{1}{m}\sum_{i=1}^{m}\left|F_{\exp} - F_{cal}\right|^2} \quad (5)$$

where m is number of data points, and $F_{\exp}$ and F_{cal} represent experimentally measured force and calculated force, respectively. To minimize the error function, the VisualDOC program[16] was combined and used with the ADAMS program[17] as shown in Fig. 10. The upper and lower bounds for stiffness were assigned 50.0N/mm and 300.0N/mm, and the upper and lower bounds for damping were assigned 0.0Ns/mm and 10.0Ns/mm for the optimization process. The VisualDOC program adopts a genetic algorithm to find the global minimum value.

The obtained stiffness and damping coefficient from the optimization routine were shown in Table 2. Since the Coulomb model could not represent the hysteretic effect, the optimized parameters with the Coulomb model could not give accurate friction force results.

Table 2. Stiffness and damping for the Coulomb friction model.

Frequency \ Displacement	0.3mm	0.5mm	1.0mm
1.0Hz	k_1=140.0 c_1=10.1	k_1=130.0 c_1=10.0	k_1=130.0 c_1=4.0
3.0Hz	k_1=140.0 c_1=3.0	k_1=130.0 c_1=2.8	k_1=130.0 c_1=2.0
6.67Hz	k_1=150.0 c_1=1.4	k_1=130.0 c_1=1.4	k_1=150.0 c_1=1.2
10.0Hz	k_1=150.0 c_1=1.0	k_1=160.0 c_1=0.4	k_1=170.0 c_1=0.3

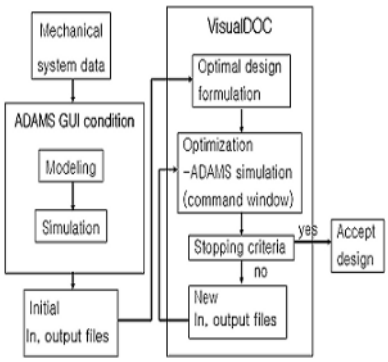

Fig. 10. Flow chart for the optimization process.

3.4 STV model

An STV (stick transition velocity) friction model shown in Fig. 11 was applied for the friction force of the sponge. The mathematical model was written as shown in Eq. (6). In the STV model, the maximum friction force increases linearly when the velocity is smaller than the STV value. If the value of the STV is zero, the STV model becomes the same as the Coulomb model. Thus, the key factor in the STV model is the magnitude of the STV value, which may depend on the frequency and amplitude of the sponge deformation.

As shown in Fig. 7, damping forces in friction damper are dependent on the external forcing frequencies. Thus, to precisely represent the hysteretic behavior, STV values should be adjusted depending on the frequency and amplitude, which is very tedious and difficult to apply in actual modeling. Thus, in the next section, an MSTV (modified stick transition velocity) model is proposed for the friction damper in which the deformation velocity of the sponge is selected for the input variable for the damper.

$$f_{fric} = \begin{bmatrix} -sign\left|\dot{X}(t)\right| f_{\max} & when \quad \left|\dot{X}(t)\right| \geq STV \\ -\dfrac{\dot{X}(t)}{STV} f_{\max} & when \quad \left|\dot{X}(t)\right| < STV \end{bmatrix} \quad (6)$$

4. Development of MSTV model

4.1 MSTV model

As shown in Fig. 7, the friction forces decrease when the exciting frequencies become higher. When the exciting frequency becomes higher, the relative velocity of sponge deformation $\left|\dot{Y}(t) - \dot{X}(t)\right|$ also becomes higher. Thus, to precisely represent the de-

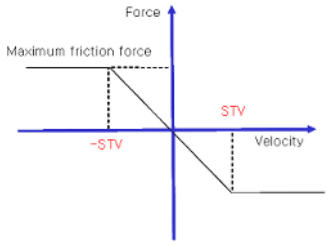

Fig. 11. STV friction model.

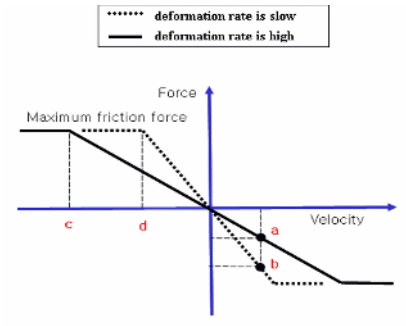

Fig. 12. MSTV friction model.

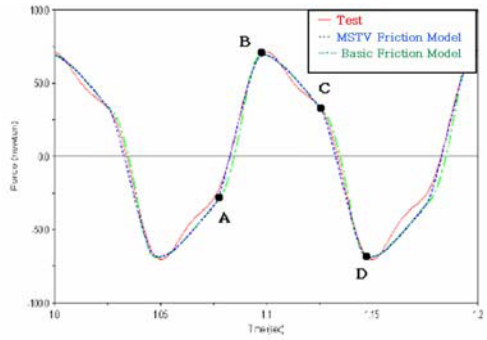

Fig. 13. MSTV model versus test (10Hz, 1.0mm).

pendency of the friction damping force on the exciting frequency, an STV model is modified to consider the relative velocity $\left|\dot{Y}(t)-\dot{X}(t)\right|$ of sponge deformation as an input variable. The friction force model for the MSTV model is shown in Eq. (7) and Fig. 12.

$$f_{fric}=\begin{bmatrix} -sign\left|\dot{X}(t)\right| f_{\max} \\ \qquad when \quad \left|\dot{X}(t)\right| \geq \left|\dot{Y}(t)-\dot{X}(t)\right| \\ -\dfrac{f_{\max}}{\left|\dot{Y}(t)-\dot{X}(t)\right|+\varepsilon}\dot{X}(t) \\ \qquad when \quad \left|\dot{X}(t)\right| < \left|\dot{Y}(t)-\dot{X}(t)\right| \end{bmatrix} \tag{7}$$

where ε is a small value to prevent to denominator becomes zero when $\left|\dot{Y}(t)-\dot{X}(t)\right|$=0.

As shown in Fig. 12, friction force depends on the relative velocity $\left|\dot{Y}(t)-\dot{X}(t)\right|$ of sponge deformation. The higher the deformation velocity becomes, the smaller friction force becomes. It means the relative velocity becomes high, so the shear force on the sponge surface becomes small.

4.2 Parameter identification for MSTV model

With the MSTV friction model shown in Fig. 12, the stiffness and damping coefficient are chosen by an optimization technique to minimize the difference between the measured data and analytical data. For the optimization, the objective function was selected the same as Eq. (5). The optimized stiffness k_1 was selected 176.0N/mm, and the damping coefficient of c_1 and c_2 are selected as 0.09Ns/mm and 0.4 Ns/mm, respectively.

With the optimized stiffness and damping coefficients in the MSTV model, the results are compared to the experimental results in Fig. 13 when the exciting frequency is 10Hz and the amplitude is 1mm. As shown in Fig. 13, regions AB and CD show very nice agreement, but regions BC and DA show relatively high error. This could be expected from the experimental data shown in Fig. 5, which shows more fluctuation in these two regions BC and DA. Although there are some deviations between experimental results and analytical results with the MSTV model, the error seems within a certain bound, which is acceptable. Thus extended comparisons were carried out for more cases.

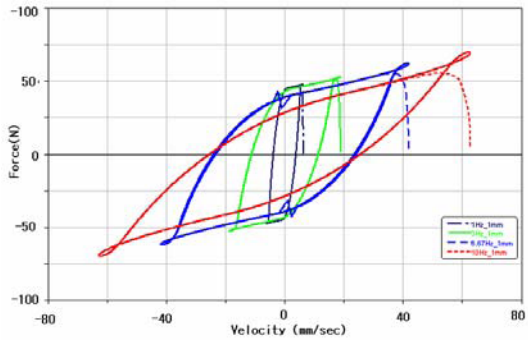

Fig. 14. Hysteretical curve with an MSTV model.

With the optimized stiffness and damping coefficients in the MSTV model, the results are also compared to the STV model in Fig. 13, in which the Basic_friction curve represents the result obtained from the MST model with MST value of 0.1mm/s. As shown in Fig. 13, an STV model shows larger error than the MSTV model in the regions of AB and CD. The hysteretic curves with an MSTV model were shown in Fig. 14, which are very similar to the experimental results shown in Fig. 7.

4.3 Accuracy of MSTV model

With the obtained stiffness and damping which are optimized for the case of 10H frequency and 1 mm of amplitude, several cases were also compared to ex-

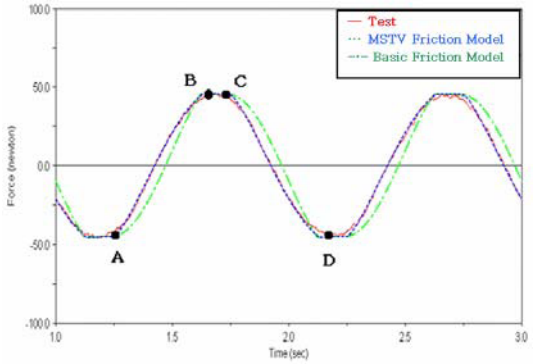

Fig. 15. Simulation versus test (1Hz, 0.3mm).

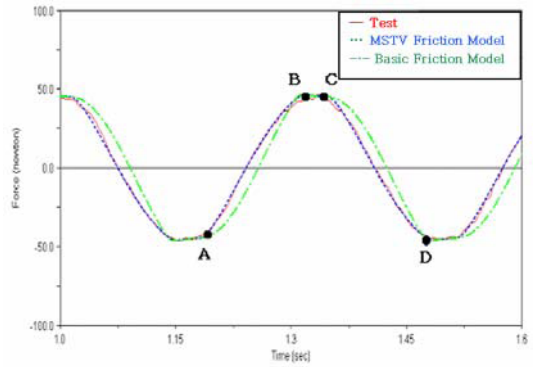

Fig. 16. Simulation versus test (3Hz, 0.3mm).

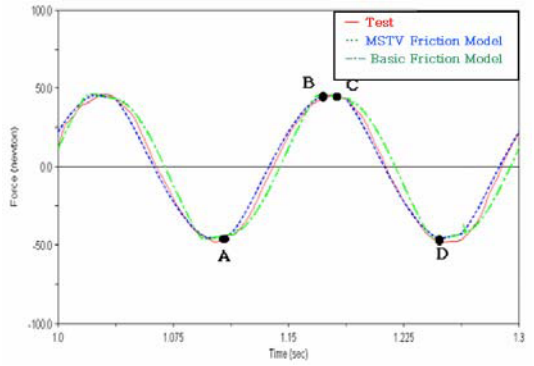

Fig. 17. Simulation versus test (6.67Hz, 0.3mm).

perimental results. Fig. 15, Fig. 16, Fig. 17, and Fig. 18 show the results of frequency 1Hz, 3Hz, 6.67Hz, and 10Hz when the amplitude is fixed to 3mm. As shown in Fig. 15 to Fig. 18, STV results show larger error than the MSTV model. When the amplitude is increased to 0.3mm, the deviation becomes larger compared to the case of 1.0mm.

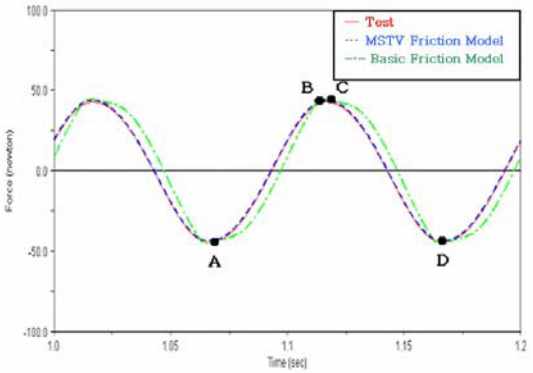

Fig. 18. Simulation versus test (10Hz, 0.3mm).

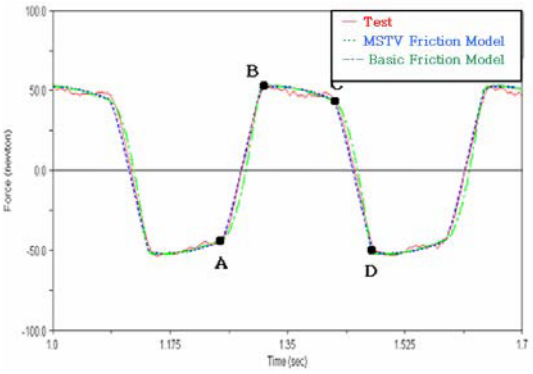

Fig. 19. Simulation versus test (3Hz, 1.0mm).

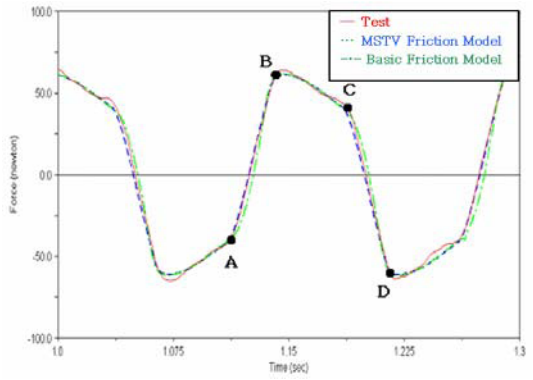

Fig. 20. Simulation versus test (6.67Hz, 1.0mm).

Fig. 19 and Fig. 20 show results of 3Hz, and 6.67Hz when the amplitude is fixed to 1.0mm. As shown in Fig. 19 and Fig. 20, regions BC and DA still show relatively high error, which seems to come from the fluctuating characteristic in the experimental data shown in Fig. 5.

5. Conclusions

In this paper, a reasonable model for a friction damper was suggested. To model the hysteretic behavior of a friction damper, a Coulomb friction model was first applied. To get a refined model for stick and transition, an STV (stick transition velocity) model was analyzed. To develop a more accurate mathematical model, an MSTV (modified stick transition velocity) model was proposed. In the MSTV model, the friction force could be changed due to the velocity of the damper, and the damping force was calculated according to the relative velocity between the external displacement and the deformation of the sponge in the friction damper. The MSTV model was in a good agreement with the experimental results.

References

[1] D. Ward, A novel remote measurement and monitoring system for the measurement of critical washing parameters inside a domestic washing machine, *Measurement*, 34 (2003) 193-205.

[2] A. Sergio et al, The design of a washing machine prototype, Materials and Design, 24 (2003) 331-338.

[3] S. Bae et al, Dynamic analysis of an automatic washing machine with a hydraulic Balancer, Journal of Sound and Vibration, 257 (1) (2002) 3-18.

[4] S. Lee et al, Vibration Analysis of a Pulsator Type Washing System, Trans. of KSNVE, 7 (2) (1997) 261-272.

[5] H. Oh and U. Lee, Dynamic Modeling and Analysis of the Washing Machine System with an Automatic Balancer, Trans. of KSME, 28 (8) (2004) 1212-1220.

[6] J. Lee, S. Jo, T. Kim and Y. Park, Modeling and Dynamic Analysis of a Front Loaded Washing Machine with Ball Type Automatic Balancer, Trans. of KSNVE, (1998) 670-682.

[7] B. Yang, J. Lee, J. Ha and B. Ahn, Optimal Design of Air Dampers Applied on Wash Machines, Trans. of KSME, 18 (9) (1994) 2477-2485.

[8] H. Han, T. Kim and T. Park, Optimal Design of a Washer using a Response Surface Method, Trans. of KSME, 23 (11) (1999) 1871-1877.

[9] J. H. Sohn, S. K. Lee, J. K. Ok and W. S. Yoo, Comparison of Semi-Physical and Black-Box Bushing Model for Vehicle Dynamics Simulation, Int. Journal of Mechanical Science and Technology, 21 (2) (2007) 264-271.

[10] B. L. Choi, J. H Choi and D. H. Choi, Reliability-Based Design Optimization of an Automotive Suspension System for Enhancing Kinematic and Compliance Characteristics, Int. Journal of Automotive Technology, 6 (3) (2005) 235-242.

[11] J. W. Liang and B. F. Feeny, Identifying Coulomb and Viscous Friction from Free-Vibration Decrements, Nonlinear Dynamics, 16 (1998) 337-347.

[12] H. Wee, Two-DOF Nonlinear System Analysis Using a Generalized Bouc-Wen Model, Proceedings of SPIE the International Society of Optical Engineering, (2000) 1692-1695.

[13] J.-K. Ok, W.-S. Yoo and J.-H. Sohn, Experimental study on the Bushing Characteristics under several excitation inputs for Bushing Modeling, Int. Journal of Automotive Technology, 8 (4) (2007) 455-465.

[14] W.-S. Yoo, K.-N. Kim, H.-W. Kim and J.-H. Sohn, Developments of Multibody ystem Dynamics: Computer Simulations and Experiments, Multibody System Dynamics, 18 (2007) 35-58.

[15] MTS, http://www.mts.com.

[16] VisualDOC User Manual, VR&D Coorp., (2004).

[17] ADAMS User Manual, MSC Software Corporation, (2003).